Spectral and redox characterization of the heme c_i of the cytochrome b_6f complex

Jean Alric*, Yves Pierre*, Daniel Picot*, Jérôme Lavergne[†‡], and Fabrice Rappaport[‡§]

*Unité Mixte de Recherche 7099, Centre National de la Recherche Scientifique-Université Paris 7, and [§]Unité Mixte de Recherche 7141, Centre National de la Recherche Scientifique-Université Paris 6, Institut de Biologie Physico-Chimique, 13 Rue Pierre et Marie Curie, 75005 Paris, France; and [†]Département d'Ecophysiologie Végétale et de Microbiologie, Unité Mixte de Recherche 6191, Centre National de la Recherche Scientifique-Commissariat à l'Energie Atomique-Aix Marseille II, Commissariat à l'Energie Atomique Cadarache, 13108 Saint Paul-lez-Durance Cedex, France

Communicated by Pierre A. Joliot, Institut de Biologie Physico-Chimique, Paris, France, September 16, 2005 (received for review June 13, 2005)

Absorption spectra of the purified cytochrome b_6f complex from *Chlamydomonas reinhardtii* were monitored as a function of the redox potential. Four spectral and redox components were identified: in addition to heme *f* and the two *b* hemes, the fourth component must be the new heme c_i (also denoted *x*) recently discovered in the crystallographic structures. This heme is covalently attached to the protein, but has no amino acid axial ligand. It is located in the plastoquinone-reducing site Q_i in the immediate vicinity of a *b* heme. Each heme titrated as a one-electron Nernst curve, with midpoint potentials at pH 7.0 of −130 mV and −35 mV (hemes *b*), +100 mV (heme c_i), and +355 mV (heme *f*). The reduced minus oxidized spectrum of heme c_i consists of a broad absorption increase centered ≈425 nm. Its potential has a dependence of −60 mV/pH unit, implying that the reduced form binds one proton in the pH 6–9 range. The Q_i site inhibitor 2-*n*-nonyl-4-hydroxyquinoline *N*-oxide, a semiquinone analogue, induces a shift of this potential by about −225 mV. The spectrum of c_i matches the absorption changes previously observed *in vivo* for an unknown redox center denoted "G." The data are discussed with respect to the effect of the membrane potential on the electron transfer equilibrium between G and heme b_H found in earlier experiments.

cytochrome bc_1 | electron transfer | quinone binding pocket | cytochrome *c*′

The cytochrome b_6f complex is one of the three membrane protein complexes composing the electron transfer chain of oxygenic photosynthesis together with the photosystem (PS) I and II reaction center complexes. It is a plastohydroquinone: plastocyanin oxidoreductase whose role is similar to that of the bacterial or mitochondrial bc_1 complex (for recent reviews, see refs. 1–3). It catalyzes the electron transfer from the lipid-soluble plastoquinol to the soluble protein plastocyanin contained in the luminal space. A part of the redox energy is used to drive an electrogenic electron/proton transfer loop that results in the translocation of one additional proton per electron from the stroma into the lumen, in accordance with the Q-cycle scheme (ref. 4 and see ref. 5 for a recent discussion of the mechanism). The oxidizing site Q_o splits the quinol electrons along two different paths. One electron goes into a high potential chain comprising the $(Fe\text{-}S)_2$ cluster of the iron sulfur protein subunit and the *c*-type heme of the cytochrome *f* subunit. These redox centers are located close to the lumen, where cytochrome *f* reacts with plastocyanin. The second electron enters a low potential chain including the two *b*-type hemes of the cytochrome b_6 subunit. This route is directed across the membrane and leads to the quinone reduction site Q_i. Accumulation of two electrons at this site allows the reduction of one plastoquinone (PQ), with two protons taken up from the stroma. Although these features are similar to those found in the bc_1 complex, the b_6f has additional functions. Evidence for a proton pumping pathway, acting in addition to the Q-cycle, has been reported (6, 7). The b_6f complex is believed to be involved not only in linear (water → PS II → b_6f → PSI → NADPH) electron transfer but also in a cyclic pathway around PS I. Thus, the complex is probably able to catalyze the reduction of quinone at the Q_i site by reduced stromal ferredoxin (for a review see ref. 8). It is also a key element in the signaling pathway designated as "state transitions." This regulation process controls the allocation of light-harvesting proteins to PS I and II and the switch between the cyclic and linear electron transfer regimes, in response to the physiological needs of the chloroplast as expressed by the redox state of the PQ pool. The Q_o site of b_6f is believed to act as the primary sensor, triggering a chain of events leading to the activation of a kinase and phosphorylation of the light-harvesting complexes (for a review see ref. 9).

Although b_6f has additional functions of its own, it was widely expected that the electron transfer cofactors were essentially homologous to those of the bc_1 complex. It therefore came as a surprise when the x-ray structure of b_6f revealed the presence of an additional heme with unusual structural properties. This heme named c_i (10) or *x* (11) is covalently attached by a single thioether bond to the conserved Cys-35 of the b_6 subunit. It thus belongs to the *c*-type family, but here, the protein provides no axial ligand to the heme iron. In general, the heme iron is hexacoordinated in cytochromes *c*, with the exception of cytochrome c_{554} (heme 2) (12) and cytochrome *c*′, both pentacoordinated. Cytochrome *c*′ is a soluble protein found in many Gram-negative bacteria (see ref. 13 for a review). Its physiological function has long remained unclear, but a role for protecting against NO has been proposed (14, 15). The *c*′-type heme has a mixed high/intermediate spin (16), and its absorption spectrum is dominated by the Soret peak in the blue region, whereas only a weak broad band appears in the green region. Heme c_i is the only known example of a cytochrome heme natively devoid of axial ligands. It is located in the Q_i pocket, inserted between the putative quinone binding site and heme b_i (we denote as b_i and b_o the *b* hemes closest to the Q_i and Q_o sites, respectively). The heme plane is almost perpendicular to that of b_i. The Fe–Fe distance between c_i and b_i is ≈9.8 Å, and the edge-to-edge distance between the hemes is even much smaller (4.7 Å). Some electronic density on the internal side of heme c_i has been ascribed to a water molecule providing weak axial ligation to the Fe. This water is expected to be H-bonded to a propionate of heme b_i. The structural information thus suggests that heme c_i must be an essential factor for quinone reduction at the Q_i site. One also expects rapid electron transfer and significant interactions between hemes c_i and b_i.

Earlier studies of the b_6f complex had provided no clue as to the involvement of an additional cofactor, with one exception. In experiments with the unicellular alga *Chlorella sorokiniana*, Lavergne (17) and Joliot and Joliot (18) reported the

Conflict of interest statement: No conflicts declared.

Abbreviations: NQNO, 2-*n*-nonyl-4-hydroxyquinoline *N*-oxide; PQ, plastoquinone; PS, photosystem; E_m, midpoint potential; r.u., relative units.

[‡]To whom correspondence may be addressed. E-mail: jerome.lavergne@cea.fr or fabrice.rappaport@ibpc.fr.

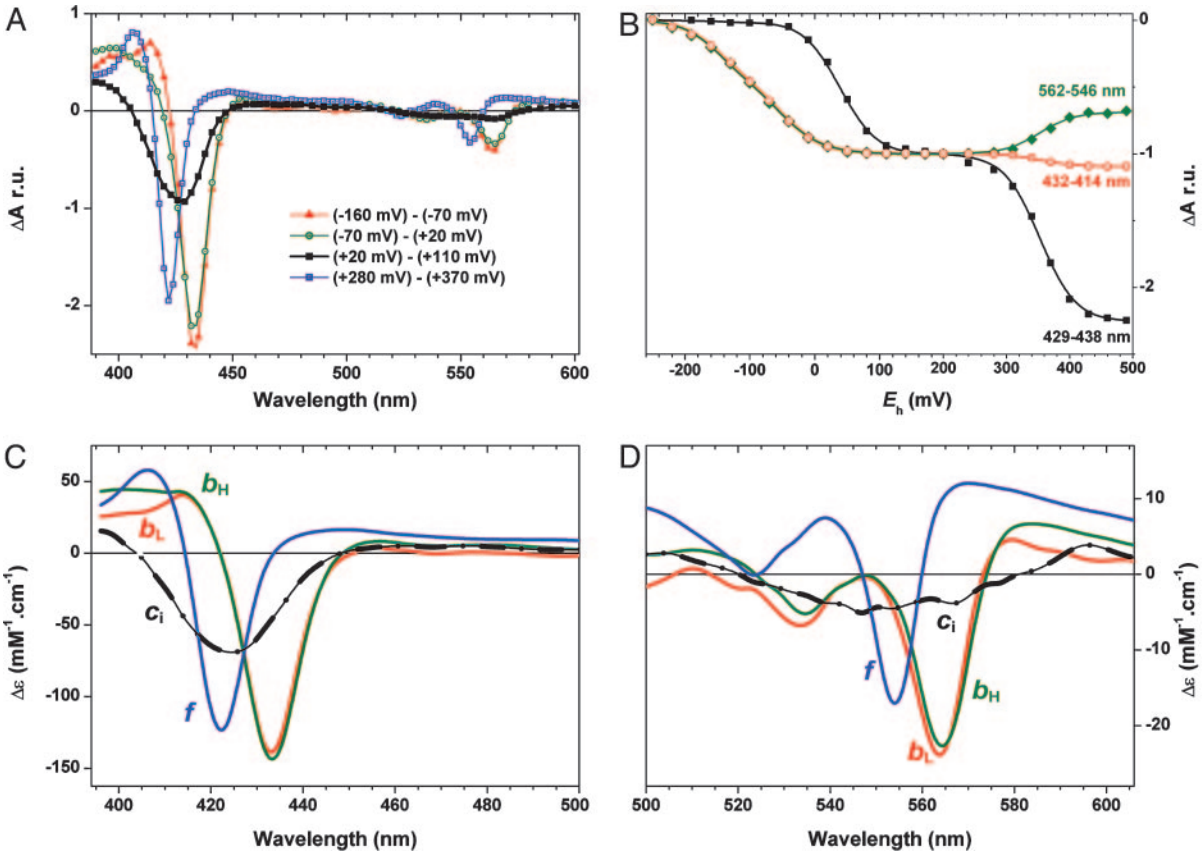

Fig. 1. Redox titration of the purified b_6f complex at pH 8 and individual difference spectra of the four hemes. (*A*) Absorption changes induced when varying the redox poise by 90-mV intervals, as indicated. (*B*) Absorption changes as a function of the applied redox potential E_h for various differences of wavelengths, as indicated. The differences (432–414 nm) and (562–546 nm) eliminate the contribution of c_i (notice that the two sets of data are superimposed in the low potential region), whereas the difference (429–438 nm) eliminates the contribution from the *b* hemes. The three plots were individually normalized to a change of 1 unit over the −250-mV to +200-mV interval. The lines are fits of the data with sums of two or three one-electron Nernst functions. The E_m values thus found were −150 ± 15 mV (b_L), −50 ± 15 mV (b_H), 40 ± 10 mV (c_i), and 355 ± 10 mV (*f*). These error bars, estimated by the fitting routine, are consistent with the scatter in independent experiments. (*C* and *D*) Oxidized minus reduced spectra of the individual components, obtained as described in the text. The vertical axis was scaled to match the $\Delta\varepsilon$ found by Metzger *et al.* (41) for cytochrome *f* in the α band region. r.u., relative units.

existence of a new redox center, which was called "G." This carrier was shown to exchange one electron with a *b* heme, with an equilibrium constant depending on the membrane potential. With untreated aerobic algae in the dark-adapted state, a fraction of the complexes appeared to have one electron in the (G/*b*) couple, with a predominance of the (G^{red}/b^{ox}) state. The effect of the light-induced membrane potential was then to shift the redox equilibrium toward *b* reduction (G^{ox}/b^{red}). The reoxidation of cytochrome *b* appeared correlated with the decay of the membrane potential and was coupled to the growth of an absorption band ≈425 nm ascribed to G. The effect of the membrane potential, promoting *b* reduction by G when the lumen is positively charged, implied that G was located closer to the stromal side than its *b* partner. Furthermore, the sensitivity and apparent linearity of this effect suggested that the *b* heme was only slightly more reducing than G [by 20–30 mV (17, 18)]. Because a large fraction of the complexes was found to contain one electron in the (G/*b*) couple under mild reducing conditions, it was proposed that the heme involved was the high potential one, b_H (presumably b_i), rather than the low potential one (b_L heme, presumably b_o). The reduced minus oxidized spectrum of G was essentially consisting of a broad absorption increase ≈425 nm, with no obvious change in the green region. On this basis, it was proposed that G could be a *c*′-type heme (18).

Clearly, the heme c_i appears as a good candidate to be identified with G. The absence of strong axial ligands may be expected to result in a high-spin or mixed-spin character, with an optical spectrum similar to that of a *c*′ heme. The heme c_i is located closer to the stromal side than b_i, so that the electrogenic character of the electron transfer between both partners is in qualitative agreement with that ascribed to the (G/*b*) couple. One goal of the present work was to determine the optical and redox properties of the heme. As will be shown, the results confirm the proposed identification with G, but also raise intriguing questions for interpreting the observations made *in vivo*.

Materials and Methods

Sample Preparation. Purification of the 6-His-tagged b_6f complex from *Chlamydomonas reinhardtii* was performed as described (10).

Optical Spectroscopy. Absorption changes were measured with a laboratory-built spectrophotometer with a xenon flash lamp as a light source (19). Laser-flash photolysis experiments were performed with a laboratory-built laser spectrophotometer (20) using the frequency-doubled 532-nm pulse from a Nd:YAG laser (5-ns duration, 10 mJ per pulse) for the photodissociation of CO.

Redox potentiometry was performed with a laboratory-built thin spectroelectrochemical cell (200-μm optical path length) similar to that described in ref. 21. The working electrode is a

thin gold grid (InterNet, Minneapolis) modified by 2-pyridinecarboxaldehyde thiosemicarbazone (Sigma) to avoid protein adsorption. A platinum counterelectrode and an Ag/AgCl reference electrode were in contact with the sample whose redox potential was clamped by a potentiostat. The sample, containing ≈10 μM of the b_6f complex, was supplemented with 100 mM KCl and buffered by 100 mM Mes (pH 6), Hepes (pH 7), or Tris (pH 8 or 9). The following redox mediators were purchased from Sigma and used at 5 μM each: potassium ferricyanide [midpoint potential ($E_{m,7}$) = +430 mV], *p*-benzoquinone (+280 mV), diaminoduiol (+341 mV), 2,5-dimethyl *p*-benzoquinone (+180 mV), phenazine methosulfate (+80 mV), ascorbate (+30 mV), duroquinone (+5 mV), menadione (0 mV), 2,5-dihydroxy-*p*-benzoquinone (−60 mV), anthraquinone (−100 mV), anthraquinone 1,5-disulfonate (−170 mV), anthraquinone 2-sulfonate (−225 mV), and benzyl viologen (−350 mV). Inhibitors of Q_i and Q_o sites, decyl-PQ (DPQ) and 2-*n*-nonyl-4-hydroxyquinoline *N*-oxide (NQNO), were purchased from Sigma. 2,4-Dinitrophenylether of iodonitrothymol was a kind gift of A. Trebst (Ruhr-University Bochum, Bochum, Germany), and tridecyl stigmatellin was synthesized as described (22).

The equilibration of the protein cofactors at the imposed redox potential was monitored from the evolution of the absorption spectrum. It was more rapidly achieved (5 min) in the high (cytochrome *f*) or low potential range (*b* hemes) than in the intermediate region (heme c_i) where it required ≈20 min. The spectral changes over a given potential change were the same in the oxidative or reductive direction.

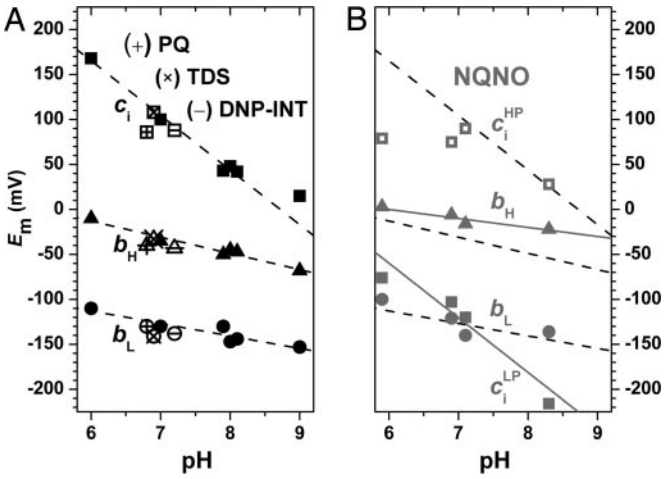

Fig. 2. Dependence on pH of the E_ms of hemes b_L (circles), b_H (triangles), and c_i (squares). (*A*) No addition (filled symbols) or at pH 7 in the presence of 300 μM decyl-PQ (PQ), 20 μM tridecyl stigmatellin (TDS), or 40 μM 2,4-dinitrophenylether of iodonitrothymol (DNP-INT). The lines are linear fits of the data yielding slopes of −60 mV/pH unit, −14 mV/pH unit, and −18 mV/pH unit for the c_i, b_H, and b_L hemes, respectively. The pH 9 data point for c_i was not taken into account because we obtained indication for a different pH dependence of this heme at pH ≥ 9. (*B*) Data in the presence of 50 μM NQNO. Same symbols as in *A*, with open and filled squares corresponding to the high (c_i^{HP}) and low potential (c_i^{LP}) titration waves of c_i, respectively. The solid gray lines are linear regressions for b_H and c_i^{LP}. The dashed lines are the same as in *A*.

Results

We recorded absorption spectra of the purified b_6f complex from *C. reinhardtii*, varying the ambient redox potential from −300 mV to +500 mV (vs. NHE). The titrations were generally started from the most reducing potential in the oxidative direction, recording the successive difference spectra with respect to the fully reduced state. It was obvious from the data, and confirmed by a global fit analysis, that four spectral components were present, titrating in distinct potential regions. Oxidation of two *b* hemes was observed in the −220-mV to 0-mV range, with two overlapping waves. Then, in the −20-mV to +100-mV range, a component characterized by a broad band ≈425 nm was observed: we ascribe this to heme c_i. Finally, the oxidation of cytochrome *f* was observed in the +220-mV to +420-mV range. Fig. 1*A* shows selected difference spectra that give a first approximation of the individual components. Fig. 1*B* shows redox titrations at pH 8, for absorption differences at selected pairs of wavelengths, which eliminate the contribution of c_i (432–414 nm and 562–546 nm), or that of the *b* hemes (429–438 nm). The lines are fits of these data with a sum of one-electron Nernst curves, yielding E_ms of −150, −50, 40, and 355 mV (at pH 8). For obtaining the spectra of the individual components shown in Fig. 1 *C* and *D*, we determined the E_ms as in Fig. 1*B* and computed the spectra from the linear system by using selected redox potential differences. A global fit routine was also used, yielding similar results. The spectra and E_Ms of the *b* hemes are roughly similar to those reported (23–27). However, we do not observe the difference in the α-band region that was found in the complex isolated from spinach, with the b_H peak at shorter wavelengths (1–2 nm) than b_L (24, 25). We actually obtained (Fig. 1*D*) a small difference (≈0.5 nm) in the opposite direction, as reported by Joliot and Joliot (18) using cells of *C. sorokiniana*. The Soret peaks also have a similar peak wavelength (434 nm), but the overshoot ≈415 nm is specific to b_L. The oxidized minus reduced spectrum of the heme c_i consists of a broad band peaking ≈425 nm with isosbestic wavelengths ≈402 and 450 nm. Although no proper α-band appears, a broad feature with a small amplitude was consistently observed in the green region. The c_i difference spectrum is similar to those reported for cytochromes *c′* (see refs. 28 and 29 for a review), although the blue band is located at a somewhat shorter wavelength (5–10 nm).

The b_6f complex possesses a chlorophyll *a* cofactor, whose red absorption band peaks ≈667 nm (27). We observed small absorption changes in this region during the redox titrations, which showed no consistent dependence on the redox potential but rather appeared caused by irreversible bleaching of the pigment. At variance with Wenk *et al.* (30), we observed no chlorophyll band shift accompanying redox changes of the *b* hemes. We also searched (exploring up to 700 nm) for a long wavelength band that would be reversibly associated with the oxidation of heme c_i and found no consistent evidence supporting this possibility. Such a long wavelength band is found in high spin hemes, although for cytochrome *c′*, the amplitude of this band is very small (29).

Similar experiments were run at various pHs from 6 to 9. We observed no significant change of the spectra of the four hemes, but their midpoint potentials did show a pH dependence, as summarized in Fig. 2*A*. The stronger pH dependence was observed for heme c_i (−60 mV/pH unit). Consistent with previous findings (26), weaker slopes were found for the *b* hemes, about −14 and −18 mV/pH unit for b_L and b_H, respectively, and cytochrome *f* showed no pH dependence between pH 7 and pH 8.

We searched for possible effects of ligands of both quinone binding sites on the spectral and redox properties of the *b* and c_i hemes. No significant effect (see the data points at pH 7 in Fig. 2*A*) was observed in the presence of 300 μM decyl-PQ, 40 μM 2,4-dinitrophenylether of iodonitrothymol (an inhibitor of the Q_o pocket; ref. 31), or 20 μM tridecy-stigmatellin, which also binds at Q_o and was cocrystallized with the complex in the x-ray work (10, 11). In contrast, the Q_i pocket inhibitor NQNO (an analogue of semiquinone; ref. 32) turned out to have dramatic and complex effects on heme c_i. Fig. 3 *A* and *B* shows the effect of NQNO (50 μM) on the redox titrations of the c_i and *b* hemes. The c_i titration (Fig. 3*A*) is now split into two waves. The low potential wave implies a shift of −225 mV (at pH 7) with respect to the control in the absence of NQNO. NQNO also caused a 20-

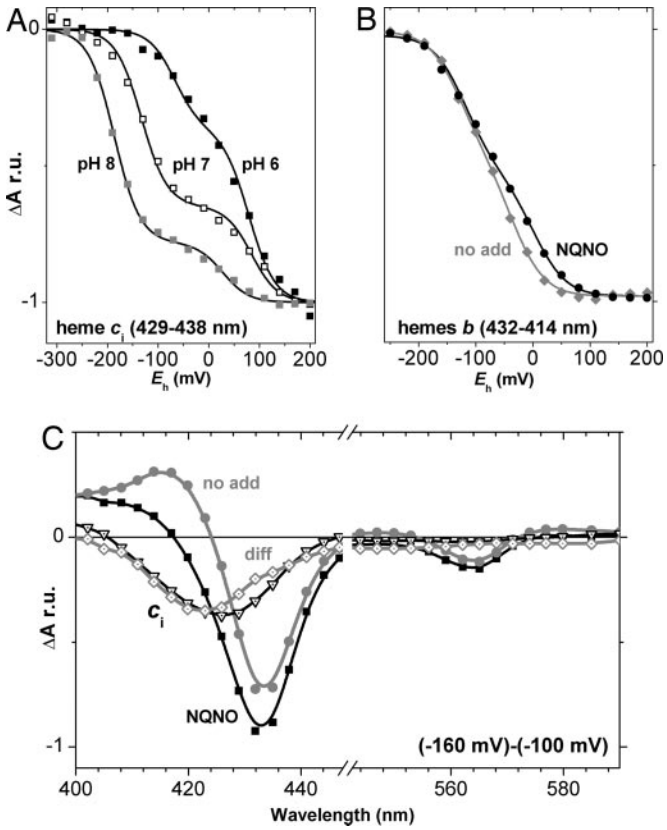

Fig. 3. Effect of NQNO on the *b* and c_i hemes. (*A*) Redox titrations of the absorption changes for the difference (429–438 nm), specific of c_i, in the presence of 50 μM NQNO, at pH 6, 7, and 8, as indicated. (*B*) Redox titration for the difference (432–414 nm), specific of the *b* hemes, in the presence or absence of 50 μM NQNO, as indicated, at pH 7. (*C*) Difference spectra over the redox potential difference −160 mV minus −100 mV, in the absence (gray circles and line) or presence (black squares and line) of 50 μM NQNO, at pH 7. The difference of these two spectra was plotted with open diamonds (it reflects the low potential wave induced by NQNO). For comparison, the open triangles show the difference obtained in the absence of NQNO over the potential difference 50 mV − 140 mV (c_i spectrum).

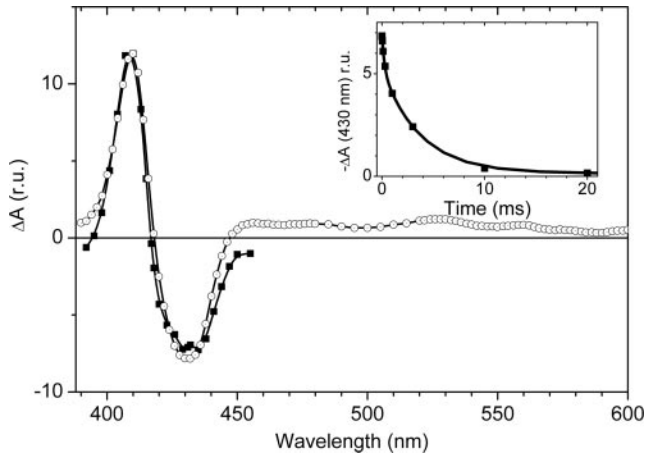

Fig. 4. Spectral changes caused by the binding of CO to the reduced b_6f complex. The open circles show the difference spectrum: (plus CO) minus (no CO). The filled squares show the spectrum of a flash-induced change measured at 40 μs, plotted with inverted sign. (*Inset*) The kinetics of recovery at 430 nm are shown (the line is a fit as a sum of two exponentials with $t_{1/2}$ = 170 μs and $t_{1/2}$ = 2.5 ms and amplitudes in the ratio 25:75). The complex was reduced by addition of a few grains of dithionite, and CO was added by bubbling.

to 30-mV increase of the E_m of heme b_H, as shown in Fig. 3*B*. Fig. 3*C* shows that the spectrum of the low potential wave induced by NQNO (diamonds) is, within experimental accuracy, the same as that of c_i in the absence of NQNO. Fig. 3*A* shows the effect of pH on the redox titration of heme c_i in the presence of NQNO. When increasing the pH, the low potential wave is shifted toward lower potentials and its relative weight increases from ≈40% at pH 6 to ≈80% at pH 8. The plot of the E_m values against the pH in the presence of NQNO is shown in Fig. 2*B*, compared with the fits obtained for the control (dashed lines). The dependence is close to −60 mV/pH unit for the low potential wave. The E_m of the high potential wave is constant below pH 7.5, but is smaller at pH 8.3, suggesting a pK_a ≈7.5 for the oxidized form of the heme. Clearly, at pH 6 and 7 the high potential wave of heme c_i in the presence of NQNO has a lower E_m and different pH dependence in comparison with the control. This finding indicates that the high potential wave does not correspond to a fraction of sites devoid of NQNO.

Cytochrome *c′* is known to bind CO in its reduced state, which is also the case for heme c_i, as reported by Zhang *et al.* (33). Fig. 4 shows the difference spectrum ± CO of a sample reduced with dithionite. Photodissociation and rebinding of the CO adduct were observed after illumination of the sample with a 532-nm laser pulse. The kinetics of the process and the spectrum of the laser-induced change (similar to the ± CO spectrum) are also shown. This difference spectrum is roughly similar to that reported in ref. 33 for the cyanobacterial complex, with a peak at 409 nm. The trough in our material is located at 430 nm rather than 424 nm, and we do not see a distinct feature ≈562 nm as described in ref. 33. The observed changes resemble those previously observed for CO binding to the cytochrome *c′* from *Chromatium* (28). The attribution of the CO binding to heme c_i is confirmed by the absence of a significant change in the green region, excluding that the binding could concern one of the other hemes.

Discussion

Heme c_i and Redox Center G. In this work, we have characterized the spectral and redox properties of the heme c_i recently discovered to be the terminal element of the low potential electron transfer chain of the b_6f complex. The oxidized minus reduced spectrum of the heme clearly confirms its identification with the redox center G described in previous work. In a preliminary report of this work (34), we used the spectra of c_i and b_H for constructing simulations of two experiments (17). The simulated families of spectra mimicked satisfactorily the experimental ones. More directly, it may be seen that the spectra obtained at long times (1–2 s) after the illumination of quinone-treated algae (figure 1 A and B in ref. 17) are close to the reduced minus oxidized spectrum of c_i.

Joliot and Joliot (18) investigated the properties of G in a mutant of *C. sorokiniana* devoid of PS II. The experiments were done under reducing conditions, observing the oxidation of the low potential chain induced by the turnover of PS I. A difference spectrum of G was constructed from such experiments. Whereas this spectrum is similar to that of c_i in the green region, it differs in the blue region where the main absorption change is observed. The proposed spectrum was an almost symmetrical band shift, with an isosbestic point at 410 nm. The procedure followed by Joliot and Joliot was to subtract two spectra (A and B). Spectrum A was contributed by the oxidized minus reduced changes of G and b_H and by the electrochromic changes induced by the membrane potential. Spectrum B, obtained in an independent experiment, contained the same extent of the electrochromic contribution and the b_L difference spectrum. The latter was used because the spectrum of b_H was not known and it was assumed

that the two spectra were very similar. As shown above, this assumption is not valid <415 nm, which is probably partly responsible for the incorrect spectrum of G in ref. 18.

Whereas the spectral properties of heme c_i and its location closer to the stromal surface with respect to heme b_i agree with the features inferred for G from the *in vivo* results, the energetic pattern in the present redox titrations is significantly different. The sensitive dependence of the redox equilibrium $(G^{red}/b^{ox}) \leftrightarrow (G^{ox}/b^{red})$ on the membrane potential requires that the difference of the E_ms be small between both partners: a $\Delta E_m \approx 20$–30 mV was thus estimated. In contrast, at pH 6.5 (as used in the experiments with algae), we found that the E_m of heme c_i is located ≈150 mV above that of b_H. An additional problem raised by the sensitivity of the response to the membrane potential is that the transmembrane distance between hemes c_i and b_i is rather small: for the Fe atoms, it amounts to ≈10% of the membrane width. Thus, one expects that, roughly speaking, the electron transfer equilibrium between the two hemes senses only ≈10% of the membrane potential (for brevity, we will call the fraction of the membrane potential felt by the two hemes their "electrogenic distance"). To quantify the observed effect, one would need an estimate of the extent of field-induced $G \rightarrow b$ electron transfer per b_6f complex. This extent could not be directly determined in ref. 17, but a quantification was obtained with respect to PS II. It was thus estimated that the membrane potential accumulated by four turnovers of the sole PS II (i.e., 100–150 mV) induced the reaction $(G^{red}/b^{ox}) \rightarrow (G^{ox}/b^{red})$ to an extent of ≈0.7 electron per PS II. The actual extent of electron transfer per complex would thus be $0.7/n$, where n stands for the b_6f/PS II stoichiometry. Denoting by ΔV the electric potential difference applied between the two partners, the fraction of (G^{ox}/b^{red}) is $1/(1 + 10^{\Delta E_m - \Delta V/60})$. This function shows that the minimum ΔV required for the displacement of $0.7/n$ electron is ≈100 mV for $n = 1$ or ≈40 mV for $n = 2$. We do not know the value of n in this material, but it is usually close to 1 and one may safely assume $n \leq 2$, which would imply a minimum electrogenic distance of (40 mV/150 mV) ≈30%. There are large error bars in these estimates, but an electrogenic distance of only 10% seems definitely too small to account for the observed effect. Further work will be needed to clarify these discrepancies between *in vivo* and *in vitro* results. In the next section, we examine some leads relevant to the issues of the electrogenic distance and the equilibrium constant between the two partners.

Electrogenic Distance. H^+ movement also must be taken into account when dealing with electrogenicity. The strongest pH dependence (about −60 mV/pH unit) was found for c_i, indicating that in the explored pH range, the reduction/oxidation of c_i is accompanied by the binding/release of one proton. Weaker dependencies (about −15 mV/pH unit) were obtained for b_H and b_L so that we ignore for simplicity the partial deprotonation associated with the oxidation of b_H. The net charge on c_i (neglecting dipolar effects) does not change, because it binds a proton when reduced. Thus, we can portray the movement of charges in the G/b equilibrium as $b^+ (GH^+) \leftrightarrow b\,(G^+) + H^+_{stroma}$. The overall change is the transfer of one positive charge from the stromal medium to b_H, which means an ≈2-fold larger electrogenic distance than that estimated from the transmembrane distance of c_i and b_H. The effect could still be larger if *in vivo* a protein partner caps the stromal surface of the complex, thus increasing the distance to the stromal medium.

Another possibility may be considered, where contrary to the arrangement found in the bc_1 complex, one would have $b_H = b_o$ and $b_L = b_i$. The electrogenic distance (from b_H to c_i or the stroma, as explained above) would then be much larger. To our knowledge, there is presently no evidence (e.g., from mutants, as was the case for the bc_1, ref. 35) that would allow an unambiguous attribution of the high and low potential hemes. Functionally, the location of b_L close to c_i would imply an uphill electron transfer step in the low potential chain ($b_H \rightarrow b_L \rightarrow c_i$), but uphill steps are not exceptional in electron transfer chains (36). We obtained however one piece of evidence suggesting that the "orthodox" location of b_H as b_i is correct, namely the 20- to 30-mV upward shift of the E_m of b_H caused by NQNO. We will discuss later the significance of this effect.

ΔE_m Between c_i and b_H. The ΔE_m obtained in the present redox titrations may not be appropriate to deal with the $c_i \leftrightarrow b_H$ electron transfer equilibrium. In our titrations, c_i is titrated in the presence of oxidized b_H and, conversely, b_H is titrated in the presence of reduced c_i, so that if any interaction is present (e.g., the oxidation of b_H shifts upward the E_m of c_i), it should be subtracted from the titration value to obtain the relevant ΔE_m for the equilibrium. Although the protonation of the reduced c_i should weaken electrostatic interactions, the proximity of the two hemes makes it likely that a significant interaction still takes place. On the other hand, it should be noted that the ΔE_m corrected from the interaction could not be very small (i.e., <40 mV), because a split titration would then be expected, with a fraction of b_H cotitrating with c_i. No such high potential wave was found for b_H, to a significant extent, as can be determined sensitively because the α band of b_H provides a specific marker. It is actually tempting to interpret the 20- to 30-mV upward shift of b_H caused by NQNO as indicative of the magnitude of the interaction between hemes c_i and b_i (b_H). Because NQNO shifts a large fraction of c_i to a low potential E_m, a corresponding fraction of b_i now titrates in the presence of oxidized c_i, contrary to the control titration. If this interpretation is correct, the ≈30-mV correction to the ΔE_m would still not be quite sufficient to settle the present issue. Another possibility is that, when investigating the c_i/b_H equilibrium *in vivo*, the E_m of c_i may be shifted downward by the presence of a semiquinone in the Q_i pocket, explaining the small equilibrium constant between c_i and b_H. In fact, we observed with NQNO, which is the analogue of a protonated semiquinone (32), a dramatic shift of the E_m of c_i, by about −225 mV, which is larger than the about −100 mV shift that would be required to account for the equilibrium observed *in vivo*.

Interestingly, in bacterial chromatophores, Shinkarev and coworkers (37) found an efficient reversed electron transfer from b_H to b_L in the bc_1 complex in response to the membrane potential generated by the reaction center. The effect was consistent with an equilibrium constant of ≈10–15 between the two hemes in the absence of membrane potential. However, the equilibrium constant expected from redox titrations ($\Delta E_m \approx 135$ mV) is rather ≈200. Shinkarev and coworkers suggested that electrostatic interactions (between the two hemes of a complex and between the two b_L hemes of a dimer) could be responsible for the ≈70-mV discrepancy. In the b_6f complex the ΔE_m between c_i and b_L is ≈260 mV (at pH 6.5), and electrostatic interactions could hardly be large enough to reduce the equilibrium constant to <10. Thus, despite the attractive analogy with the bc_1 complex, it is unlikely that the b heme involved in the G/b equilibrium observed *in vivo* is b_L. This equilibrium might, however, span the entire low potential chain if, as considered above, it turned out that $b_H = b_o$.

Ligands to the Quinone Pockets. Two ligands appeared to affect heme c_i. CO caused a spectral modification of the reduced heme akin to that observed in c'-type cytochromes. We have no data on the effect of CO on the midpoint potential of c_i, although it is very likely that it induces a large upward shift. Such a shift is related to the greater affinity of CO to a reduced form of the heme (38). An inhibitory effect of CO for the electron exchange between G and b_H in *vivo* was reported in ref. 18. NQNO caused no obvious change of the oxidized minus reduced spectrum of c_i,

but it did affect its redox properties. The titration was split into two waves, both (for pH < 7.5) at lower potential than the control. The low potential wave retained the -60 mV/pH unit dependence of the control but was downshifted by 235 mV. A smaller effect in the same direction was reported for the binding of NQNO to a *b* heme of formate dehydrogenase (ref. 39 but see also ref. 40). A decreased E_m is thermodynamically equivalent to a stronger binding to the oxidized form of the heme. The observed $\Delta E_m = -225$ mV (low potential wave) in the presence of 50 μM NQNO implies that the dissociation constant for the oxidized heme is in the nM range or below and becomes >6,500-fold larger for the reduced form (see *Appendix*, which is published as supporting information on the PNAS web site). It is thus possible that, under our experimental conditions, NQNO was actually released from the Q_i site upon reduction of c_i. As emphasized in the *Appendix*, the appearance of two titration waves is not caused by the different affinity depending on the redox state of the heme, which predicts a shifted but homogeneous titration. It must reflect the presence of two forms of the complex. A sample heterogeneity proper is unlikely because the relative amplitude of the two titration waves of c_i in the presence of NQNO is pH-dependent, which rather suggests an equilibrium between two conformations. The protonation state of the complex would then control the differential affinity for NQNO of the reduced/oxidized forms of c_i. We feel that these effects may be indicative of a reorganization of the Q_i pocket controlled by the redox state of the heme c_i.

Conclusion

The emergence of a quite unusual structure for the Q_i pocket of the b_6f complex raises interesting questions. It is not clear whether this arrangement evolved in relation with the specific functions of this complex with respect to the bc_1 (common) ancestor. Alternatively, it may represent an adaptation/improvement of the Q_i pocket concerning its usual role as the terminal element of the low potential chain in the Q-cycle scheme. In the present study, we have established the connection between earlier functional observations *in vivo* (the G/*b* equilibrium modulated by the membrane potential) and the characterization of the heme c_i in the purified complex. Interestingly, new questions arise, because the behavior observed *in vivo* is not entirely explained by the structural and redox information gained on the complex. More generally, further studies will have to clarify the role of the two hemes (c_i and b_i) in the mechanism of PQ reduction in the b_6f complex.

We thank J.-L. Popot and F. Zito for stimulating discussions. This work was supported by Commissariat à l'Energie Atomique, Centre National de la Recherche Scientifique, a postdoctoral fellowship from Centre National de la Recherche Scientifique (to J.A.), and the Biologie Cellulaire, Moleculaire, et Structurale Program (Grant 045552).

1. Cramer, W. A., Zhang, H., Yan, J., Kurisu, G. & Smith, J. L. (2004) *Biochemistry* **43,** 5921–5929.
2. Crofts, A. R. (2004) *Annu. Rev. Physiol.* **66,** 689–733.
3. Darrouzet, E., Cooley, J. W. & Daldal, F. (2004) *Photosynth. Res.* **79,** 25–44.
4. Mitchell, P. (1975) *FEBS Lett.* **59,** 137–139.
5. Osyczka, A., Moser, C. C. & Dutton, P. L. (2005) *Trends Biochem. Sci.* **30,** 176–182.
6. Joliot, P. & Joliot, A. (1998) *Biochemistry* **37,** 10404–10410.
7. Deniau, C. & Rappaport, F. (2000) *Biochemistry* **39,** 3304–3310.
8. Arnon, D. I. (1995) *Photosynth. Res.* **46,** 47–71.
9. Wollman, F. A. (2001) *EMBO J.* **20,** 3623–3630.
10. Stroebel, D., Choquet, Y., Popot, J. L. & Picot, D. (2003) *Nature* **426,** 413–418.
11. Kurisu, G., Zhang, H., Smith, J. L. & Cramer, W. A. (2003) *Science* **302,** 1009–1014.
12. Iverson, T. M., Arciero, D. M., Hsu, B. T., Logan, M. S., Hooper, A. B. & Rees, D. C. (1998) *Nat. Struct. Biol* **5,** 1005–1012.
13. Meyer, T. E. & Kamen, M. D. (1982) *Adv. Protein Chem.* **35,** 105–212.
14. Cross, R., Aish, J., Paston, S. J., Poole, R. K. & Moir, J. W. (2000) *J. Bacteriol.* **182,** 1442–1447.
15. Mayburd, A. L. & Kassner, R. J. (2002) *Biochemistry* **41,** 11582–11591.
16. Fujii, S., Yoshimura, T., Kamada, H., Yamaguchi, K., Suzuki, S., Shidara, S. & Takakuwa, S. (1995) *Biochim. Biophys. Acta* **1251,** 161–169.
17. Lavergne, J. (1983) *Biochim. Biophys. Acta* **725,** 25–33.
18. Joliot, P. & Joliot, A. (1988) *Biochim. Biophys. Acta* **933,** 319–333.
19. Joliot, P., Béal, D. & Frilley, B. (1980) *J. Chim. Phys.* **77,** 209–216.
20. Béal, D., Rappaport, F. & Joliot, P. (1999) *Rev. Sci. Instrum.* **70,** 202–207.
21. Baymann, F. & Rappaport, F. (1998) *Biochemistry* **37,** 15320–15326.
22. Höffle, G., Kunze, B., Zorzin, C. & Reichenbach, H. (1984) *Liebigs Ann. Chem.* **12,** 1883–1904.
23. Stuart, A. L. & Wasserman, A. R. (1973) *Biochim. Biophys. Acta* **314,** 284–297.
24. Clark, R. D. & Hind, G. (1983) *Proc. Natl. Acad. Sci. USA* **80,** 6249–6253.
25. Nitschke, W., Hauska, G. & Crofts, A. R. (1988) *FEBS Lett.* **232,** 204–208.
26. Kramer, D. M. & Crofts, A. R. (1994) *Biochim. Biophys. Acta* **1184,** 193–201.
27. Pierre, Y., Breyton, C., Kramer, D. & Popot, J.-L. (1995) *J. Biol. Chem.* **49,** 29342–29349.
28. Cusanovich, M. A. & Gibson, Q. H. (1973) *J. Biol. Chem.* **248,** 822–834.
29. Pettigrew, G. W. & Moore, G. R. (1987) *Cytochromes c: Biological Aspects* (Springer, Berlin).
30. Wenk, S. O., Schneider, D., Boronowsky, U., Jager, C., Klughammer, C., de Weerd, F. L., van Roon, H., Vermaas, W. F., Dekker, J. P. & Rogner, M. (2005) *FEBS J.* **272,** 582–592.
31. Lam, E. (1984) *FEBS Lett.* **172,** 255–260.
32. Musser, S. M., Stowell, M. H., Lee, H. K., Rumbley, J. N. & Chan, S. I. (1997) *Biochemistry* **36,** 894–902.
33. Zhang, H., Primak, A., Cape, J., Bowman, M. K., Kramer, D. M. & Cramer, W. A. (2004) *Biochemistry* **43,** 16329–16336.
34. Rappaport, F., Pierre, Y., Picot, D. & Lavergne, J. (2004) in *Photosynthesis: Fundamental Aspects to Global Perspective*, eds. van der Est, A. & Bruce, D. (Allen Press, Montreal), Vol. 1, pp. 418–420.
35. Yun, C. H., Crofts, A. R. & Gennis, R. B. (1991) *Biochemistry* **30,** 6747–6754.
36. Page, C. C., Moser, C. C., Chen, X. & Dutton, P. L. (1999) *Nature* **402,** 47–52.
37. Shinkarev, V. P., Crofts, A. R. & Wraight, C. A. (2001) *Biochemistry* **40,** 12584–12590.
38. Boelens, R. & Wever, R. (1979) *Biochim. Biophys. Acta* **547,** 296–310.
39. Kroger, A., Winkler, E., Innerhofer, A., Hackenberg, H. & Schagger, H. (1979) *Eur. J. Biochem.* **94,** 465–475.
40. Smirnova, I. A., Hägerhäll, C., Konstantinov, A. A. & Hederstedt, L. (1995) *FEBS Lett.* **359,** 23–26.
41. Metzger, S. U., Cramer, W. A. & Whitmarsh, J. (1997) *Biochim. Biophys. Acta* **1319,** 233–241.